

Poly(BODIPY)s: A New Class of Tunable Polymeric Dyes

Fikri E. Alemdaroglu,^{†,§} Seth C. Alexander,[†] Dongmei Ji,[‡] Deepak K. Prusty,[†] Michael Börsch,^{*,‡} and Andreas Herrmann^{*,†}

[†]Zernike Institute for Advanced Materials, Department of Polymer Chemistry, University of Groningen, Nijenborgh 4, 9747 AG Groningen, The Netherlands, and [‡]Physikalisches Institut, Universität Stuttgart, Pfaffenwaldring 57, 70550 Stuttgart, Germany. [§]Current address: Elastogran GmbH, Elastogranstr. 60, 49448 Lemförde, Germany.

Received April 3, 2009; Revised Manuscript Received July 30, 2009

ABSTRACT: We present a new class of polymeric dyes bearing the difluoroboraindacene (BODIPY) chromophore within the main chain. Starting from a diiodinated BODIPY monomer, homo- and copolymers with a fully conjugated backbone were efficiently synthesized by transition-metal-catalyzed polycondensation reactions. The photophysical properties of the resulting polymeric materials were investigated in bulk and at the single molecule level. It was found that the BODIPY homopolymer resembles the absorption and emission properties of the individual BODIPY chromophore. In contrast, the copolymer products of 1,4-diethynylbenzene and benzene exhibit absorption and emission spectra that are shifted hypsochromically and bathochromically in regard to the homopolymer, respectively, allowing for easy color tuning by the choice of comonomers. The fluorescence quantum yield of the BODIPY homopolymer is remarkably high (57%). The exceptional brightness of the materials was confirmed in the single molecule investigations; the BODIPY homopolymer emitted several times more photons than the well-established fluorescent probe Rhodamine 6G with a quantum yield close to unity.

Introduction

Polymeric dyes are defined as macromolecules that exhibit chemical linkages to their chromogenic units. The dyes can either be attached as side chains or incorporated into the polymer backbone. Initially, these materials were chiefly employed for coloring textile fibers and plastics. The main advantages of such macromolecular dyes compared to their low-molecular-weight counterparts are the homogeneity of the resulting colored material and the high migration fastness.¹ With the advent of organic electronics, polymeric dyes have experienced a renaissance since low migration, enhanced processability, especially good film-forming properties, and the possibility of combinations with conjugated polymers offer new opportunities for active materials within devices. One chromophore that has frequently been covalently combined with polymers is perylene. Perylene derivatives have been incorporated as pendant side chains in poly(methyl methacrylate),² poly(isocyanide),³ poly(fluorene),⁴ and poly(fluorene-*alt*-phenylene).⁵ The same chromophore has also been used as a constituent component of the main chain in poly(ethylene)⁶ and poly(fluorene).⁷ Moreover, several main-chain homopolymers of perylene derivatives have been fabricated,^{8,9} and polymeric perylenes have been employed in organic light-emitting diodes (OLEDs)⁷ and organic photovoltaics (OPVs).¹⁰ In view of this success, the search for polymeric dyes containing other chromophores continues. Polymeric cyanine dyes are one recent example of this. These fully conjugated materials absorb solely in the near-infrared region with maxima at up to 1002 nm and were envisaged for applications in OPV devices in combination with C₆₀.¹¹ Other colorants that have been directly converted into π -conjugated poly(arylene)s include indigo,¹² triarylmethane,¹³ and porphyrin.¹⁴ The polymerization of the latter resulted in linear chains that were proposed to serve as conjugated wires in molecular electronics.¹⁴

In contrast, “porphyrin’s little sister”, difluoroboraindacene (BODIPY) dyes, have only very rarely been transformed into polymeric dyes.^{15–17} The first BODIPY derivative was synthesized 40 years ago.¹⁸ Since then, these dyes have been well established for the purpose of biological labeling because of their remarkable properties, including high absorption coefficients, narrow emission bands, high quantum yields of the singlet emitter, negligible formation of the triplet state, and high photostability.¹⁹ In recent years, BODIPY dyes have also been employed for organic electronics, for instance in OLED applications.²⁰

In this contribution, the possibility of generating polymeric BODIPY dyes is explored. Different homo- and alternating copolymers containing the 4-bora-3a,4a-diaza-*s*-indacene scaffold were synthesized by various polycondensation methods, and the photophysical properties of these novel polymeric dyes were investigated in bulk and on the single molecule level.

Materials and Methods

¹H NMR and ¹³C NMR spectra were recorded in deuterated dichloromethane on a Bruker 250 and a Bruker 500 spectrometer using the residual proton resonance or the carbon signal of the solvent as the internal standard. UV and fluorescence spectra were obtained on a SpectraMax M2 instrument (Molecular Devices) at room temperature with dichloromethane, ethanol, or tetrahydrofuran (THF) as the solvent. Quantum yield measurements were carried out against the standard Rhodamine B in ethanol.²¹ Mass spectra were obtained using a field-desorption (FD) mass spectrometer (Fisons Instruments VG ZAB2-SE-FPD Sectorfield MS) or MALDI-TOF mass spectrometer (Bruker time-of-flight MS Reflex III). Gel permeation chromatography (GPC) was carried out using Soma UV/ERC RI detector with the wavelength set to the λ_{max} of the corresponding polymer and a pump from Waters Corp. All starting materials were purchased from Aldrich, Acros, ABCR, or Lancaster and were used as received.

A confocal inverted microscope in epifluorescence configuration (IX71, Olympus) was used for single-molecule fluorescence

*Corresponding authors. E-mail: m.boersch@physik.uni-stuttgart.de (M.B.), a.herrmann@rug.nl (A.H.).

spectroscopy.^{22,23} Three-dimensional sample scanning was achieved with an x - y piezo scanner combined with an objective positioner driven by a digital controller (Physik Instrumente). Several laser sources for pulsed and continuous excitation at $\lambda = 488$ nm (PicoTA 490, Picoquant; argon ion laser model 2020, Spectra-Physics) or 532 nm (Compass 315M, Coherent) were available.^{24,25} A water immersion objective (UPlanSApo 60 \times , 1.2 N.A., Olympus) focused the attenuated laser beams into the polymer solutions in toluene or onto the surface-attached single molecules. To avoid evaporation of the organic solvent, we used a 10 μ m thin chamber of three-well microscopic slides (ERIE Scientific Co.) sealed by a cover glass. Fluorescence was split by two consecutive dichroic mirrors and interference filters (AHF) into three spectral regions and detected simultaneously by three avalanche photodiodes (SPCM AQR-14, Perkin-Elmer). For solution experiments, photons were recorded with TCSPC electronics (SPC-630, Becker & Hickl). Fluorescence lifetimes and autocorrelation functions were calculated by the software "Burst-analyzer".²⁶ Single-molecule images were obtained using a programmable multichannel counter card (NI-PCI-6602, National Instruments) for the photodiode signals, used to position the piezo scanners. Spectrally resolved image analysis was performed using the custom-made software "ODA-analyzer" (N. Zarrabi, Universität Stuttgart).

Synthesis of 3. In a 100 mL round-bottom flask, 1.7 g (10.5 mmol) of 4-*tert*-butylbenzaldehyde and 2.0 g (21.0 mmol) of 2,4-dimethylpyrrole were dissolved in 12 mL of dichloromethane. 0.1 mL of trifluoroacetic acid was added to this mixture, resulting in the evolution of a gas and notable red color change. The reaction was monitored by TLC to determine reaction completion. The crude mixture was washed with 0.1 M NaCl and dried over MgSO₄. The solvent was removed in vacuo. The resulting crude product was purified by aluminum oxide column chromatography using dichloromethane as the mobile phase to give a purple powder as compound **3**; 70% yield. RF (silica TLC, CH₂Cl₂) 0.9. ¹H NMR (CD₂Cl₂, 250 MHz): $\delta = 7.21$ (d, 2H), 6.97 (d, 2H), 5.56 (s, 1H), 5.24 (s, 2H), 2.42 (s, 6H), 1.30 (s, 6H), 1.22 (s, 9H). ¹³C NMR (CD₂Cl₂, 62.5 MHz): $\delta = 163.7$, 150.0, 140.8, 128.7, 128.3, 127.4, 126.3, 115.5, 109.1, 37.2, 35.2, 32.3, 13.5, 11.6. FD MS = 335.0. Anal. Calcd for C₂₃H₃₀N₂ ($M_r = 334.5$): C, 82.59; H, 9.04; N, 8.37. Found: C, 82.66; H, 9.11; N, 8.69.

Synthesis of 4. In a 250 mL round-bottom flask, 1.5 g (4.48 mmol) of **3** was dissolved in 50 mL of toluene. 1.1 g (4.48 mmol) of tetrachloro-*p*-benzoquinone was added to this solution. After 30 min the reaction was stopped after verification by TLC. To this crude mixture, 4.37 mL (31.36 mmol) of triethylamine and 2.75 mL (22.4 mmol) of boron trifluoride diethyl etherate were added, and the mixture was allowed to react for 4 h. The reaction mixture was then placed on the rotary evaporator to remove toluene. The residual material was dissolved in a minimal amount of dichloromethane and was separated by silica gel column chromatography with dichloromethane as the mobile phase. Product **4** was eluted as the second colored compound. The yield of the reaction was 11%. RF (silica TLC, dichloromethane) 0.5. ¹H NMR (CD₂Cl₂, 250 MHz): $\delta = 7.42$ (d, 2H), 7.11 (d, 2H), 5.91 (s, 2H), 2.42 (s, 6H), 1.30 (s, 6H), 1.27 (s, 9H). ¹³C NMR (CD₂Cl₂, 62.5 MHz): $\delta = 155.7$, 153.2, 144.2, 143.4, 132.2, 128.2, 126.5, 121.8, 35.5, 31.8, 15.0, 14.8. FD MS = 380.4. Anal. Calcd for C₂₃H₂₇BF₂N₂ ($M_r = 380.28$): C, 72.64; H, 7.16; N, 7.37. Found: C, 72.55; H, 7.21; N, 7.57. UV (CH₂Cl₂) $\lambda_{\max}(\epsilon) = 500$ nm (47 000 M⁻¹ cm⁻¹). Fluorescence (excitation at 500 nm) emission_{max} = 513 nm. Quantum yield (EtOH, excitation at 498 nm) = 0.71.

Synthesis of 5. A 250 mL round-bottom flask was first charged with 1.3 g (3.42 mmol) of **4** dissolved in 40 mL of ethanol. To this solution 2.17 g (8.55 mmol) of I₂ was added and allowed to dissolve. 1.2 g (6.84 mmol) of HIO₃ was dissolved in a minimal amount of water, and this solution was added dropwise by a syringe over a 10 min time interval. After the addition was complete, the solution was heated to 60 °C and refluxed for 1 h.

The progress of the reaction was followed by TLC until completion. Ethanol was removed in vacuo, and the remaining water and solid product were worked up in dichloromethane to separate the water from the organic material. This organic layer was then reduced by a rotary evaporator, and the residue was purified by column chromatography with a silica gel solid phase and dichloromethane as the eluting solvent. The product **5** was collected as the first fraction resulting in a 60% yield. RF (silica TLC, dichloromethane) 0.9. ¹H NMR (CD₂Cl₂, 250 MHz): $\delta = 7.46$ (d, 2H), 7.18 (d, 2H), 2.51 (s, 6H), 1.32 (s, 6H), 1.29 (s, 9H). ¹³C NMR (62.5 MHz): $\delta = 157.1$, 153.9, 132.2, 128.2, 127.1, 85.0, 35.2, 31.7, 30.5, 17.5, 16.5. FD MS = 632.1. Anal. Calcd for C₂₃H₂₅BF₂I₂N₂ ($M_r = 632.02$): C, 43.70; H, 3.99; N, 4.43; B, 1.71; F, 6.01; I, 40.15. Found: C, 43.88; H, 4.11; N, 4.23; B, 1.51; F, 5.89; I, 40.21. UV (THF) $\lambda_{\max}(\epsilon) = 530$ nm (45 400 M⁻¹ cm⁻¹). Fluorescence (excitation at 530 nm) emission_{max} = 544 nm. Quantum yield (EtOH, excitation at 530 nm) = 0.02.

Synthesis of P1. In a glovebox under nitrogen atmosphere, a dry 100 mL round-bottom flask with stir bar was charged with 296 mg (1.075 mmol) of bis(1,5-cyclooctadiene)nickel(0), 116 mg (1.075 mmol) of cyclooctadiene, and 168 mg (1.075 mmol) of pyridine in 6.0 mL of a 1:1 mixture of toluene and dimethylformamide (DMF). A deep, dark purple color then developed. This flask was sealed with a rubber septum, taken out of the glovebox, and placed on a reflux condenser charged with an argon atmosphere. The solution was heated to 60 °C. In the glovebox, a dry 50 mL flask was charged with 283 mg (0.448 mmol) of the monomer **5** in 3.0 mL of a 1:1 mixture of toluene and DMF. This flask was sealed with a rubber septum and removed from the glovebox. The monomer was then syringed into the catalyst mixture preheated to 60 °C. The flask containing this solution was covered with foil to protect it from light and the reaction mixture was refluxed for 4 days. The product was precipitated in 20 mL of a 1:1 mixture of methanol and concentrated hydrochloric acid. The polymer was dissolved in dichloromethane and washed with aqueous 1.0 M sodium thiosulfate solution (3 \times 10 mL) followed by washing with Milli-Q water and drying over MgSO₄, for the removal of residual iodine from **P1**. The polymer **P1** was collected as a solid with a yield of 95%. P_n (by GPC RI) = 74. ¹H NMR (CD₂Cl₂, 250 MHz): $\delta = 7.51$ (d, 2H), 7.19 (d, 2H), 2.50 (s, 6H), 1.31 (s, 6H), 1.23 (s, 9H). ¹³C NMR (CD₂Cl₂, 175 MHz): $\delta = 143.9$, 139.2, 132.2, 131.9, 127.9, 127.2, 126.9, 126.3, 121.4, 33.1, 32.3, 31.4, 30.0, 23.1, 19.8, 14.2. UV (THF) $\lambda_{\max}(\epsilon) = 503$ nm (475 000 M⁻¹ cm⁻¹). Fluorescence (excitation at 502 nm) emission_{max} = 510 nm. Quantum yield (THF, excitation at 502 nm) = 0.57. GPC (DMF, 60 °C, UV 500 nm): $M_w = 77 600$, $M_n = 22 300$, $D(M_w/M_n) = 3.48$.

Synthesis of P2. To an argon-filled 100 mL round-bottom flask containing 338 mg (0.535 mmol) of the monomer **5**, 67 mg (0.535 mmol) of the comonomer 1,4-diethynylbenzene was added. Both compounds were dissolved in 15 mL of a 1:1 mixture of toluene and piperidine. 1 mg (1 mol %) of copper iodine and 4 mg (1 mol %) of (PPh₃)₂Pd(II)Cl₂ were added to this solution. The reaction was carried out for 4 days at room temperature. The crude mixture was then concentrated in vacuo and dissolved in a minimal amount of dichloromethane. Large amounts of methanol were then added to this mixture to precipitate the polymer. The precipitate was separated by centrifugation and the product **P2** was obtained in 80% yield. $P_n = 23$. ¹H NMR (CD₂Cl₂, 500 MHz): $\delta = 7.8$ –7.1 (broad, 8H), 1.4–0.9 (broad, 21H). ¹³C NMR (CD₂Cl₂, 175 MHz): $\delta = 164.1$, 152.5, 148.7, 140.6, 137.1, 135.3, 132.9, 129.3, 125.2, 123.6, 118.7, 116.6, 111.4, 108.4, 92.3, 86.1, 83.6, 77.2, 32.1, 15.7, 13.1. UV (THF) $\lambda_{\max}(\epsilon) = 325$ nm (107 500 M⁻¹ cm⁻¹). Fluorescence (excitation at 325 nm) emission_{max} = 385 nm. Quantum yield (THF, excitation at 325 nm) = 0.02. GPC (THF, 30 °C, RI): $M_w = 30 600$, $M_n = 9700$, $D(M_w/M_n) = 3.15$.

Synthesis of P3. A 100 mL round-bottom flask was charged with an argon atmosphere, 238 mg (0.377 mmol) of monomer **5**,

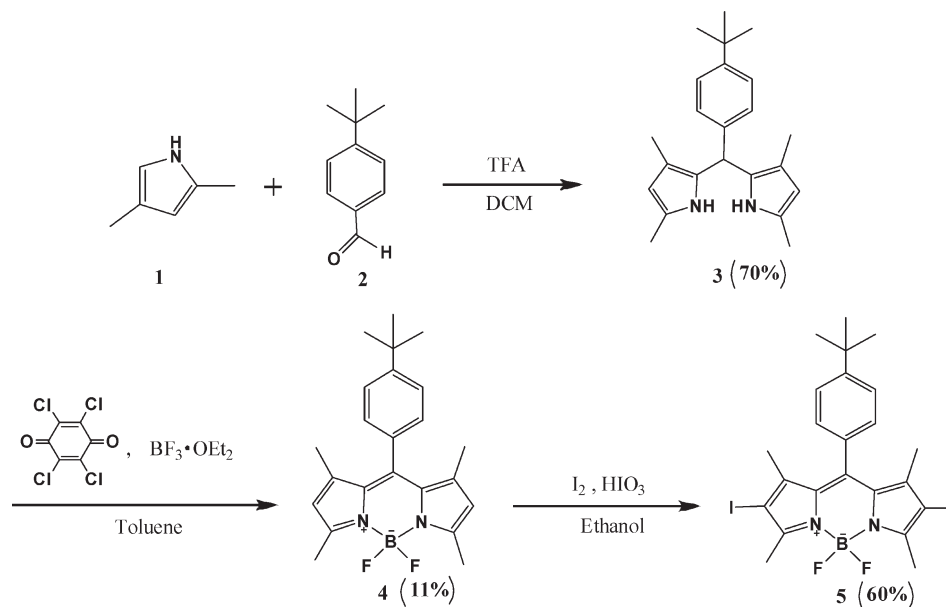


Figure 1. Synthetic route to the BODIPY monomer.

62 mg (0.377 mmol) of benzene-1,4-diboronic acid, and 28 mL of a 2.5:1 mixture of THF/H₂O. Next, 586 mg (6.97 mmol) of sodium bicarbonate was added, followed by 3 mg (0.7 mol %) of the (PPh₃)₄Pd(0) catalyst. The reaction mixture was placed under a reflux condenser, purged with argon, and heated to reflux for 4 days. The crude reaction mixture was cooled and THF was removed in vacuo. After filtration, the dry solid was dissolved in a minimal amount of dichloromethane and precipitated with copious amounts of methanol. The precipitate was separated by centrifugation which yielded 23% of polymer **P3**. P_n (by GPC RI) = 16. ¹H NMR (CD₂Cl₂, 500 MHz): δ = 7.67–7.12 (broad, 8H), 1.44–1.21 (broad, 21H). ¹³C NMR (CD₂Cl₂, 175 MHz): δ = 150.7, 149.6, 138.5, 108.5, 58.0, 54.4, 53.0, 45.9, 40.0, 39.1, 37.1, 35.8, 24.1, 22.8. UV (THF) λ_{max} (ϵ) = 535 nm (20 000 M⁻¹ cm⁻¹). Fluorescence (excitation at 535 nm) $\text{Emission}_{\text{max}}$ = 575 nm. Quantum yield (THF, excitation at 535 nm) = 0.24. GPC (THF, 30 °C, RI): M_w = 19 300, M_n = 6400, D (M_w/M_n) = 3.02.

Removal of Residual Pd Catalyst. It would be essential to remove palladium nanoparticles, the degraded product of the catalyst, from the crude polymer materials before any application in an electroactive device. There have been a few reports on the removal of residual palladium from polymers,^{27,28} but there has been no successful method for achieving complete metal elimination. We attempted to remove the palladium contamination using a reported approach for our polymer products **P2** and **P3**.²⁸ To a solution of the polymer (typically 10 mg/1 mL sample) in chloroform, *N,N*-diethyldithiocarbamate was added, and the solution was stirred for 1 h, followed by precipitation of the polymer in methanol and repeated washing with methanol. The polymer was then dried in a vacuum oven. No palladium was found from the elemental analysis results for polymers **P2** and **P3** which indicates that the remaining catalyst content is below 0.0001% w/w.

Results and Discussion

Metal-catalyzed homo- and cross-coupling reactions have been established as powerful tools to prepare high molecular weight materials, especially polyarylenes.²⁹ A simple method to produce conjugated polymers is the Yamamoto reaction, which just requires a dihalide-functionalized aromatic monomer and stoichiometric quantities of a nickel complex.³⁰ Alternatively, the Suzuki coupling³¹ or the Hagihara–Sonogashira reaction³² can

be employed to synthesize aromatic polymers. For these two methods a second monomer is required, either an aryldiboronic acid derivative or a diethynyl compound, respectively, that reacts in the presence of a transition metal catalyst with the dihalogenated monomer in an AABB-type polycondensation. As we were interested in incorporating BODIPY in the main chain of the polymer, at the very least a dihalide-substituted dipyrrometheneboron scaffold was required.

Synthesis of Monomer. For the generation of the symmetrical BODIPY monomer the well-known pyrrole condensation method was employed (Figure 1). 2,4-Dimethylpyrrole (**1**) was reacted with 4-*tert*-butylbenzaldehyde (**2**) in the presence of trifluoroacetic acid to form the dye precursor **3**. The utilization of **1** carrying a methyl group adjacent to the nitrogen atom prevented oligomerization or porphyrin formation. The bulky alkyl group within aldehyde **2** was chosen to increase the solubility, especially important since we envisaged macromolecules consisting of extended aromatic cores. The BODIPY dye **4** was obtained after treatment with tetrachloro-*p*-benzoquinone acting as an oxidizing agent and complexation with boron trifluoride diethyl etherate. To introduce two halogen atoms in the remaining 2- and 6-positions of the diazaindacene scaffold to allow subsequent polycondensation reactions, **4** was reacted with a mixture of iodine and iodic acid to yield the BODIPY monomer **5**.

Synthesis of Polymers. First the monomer **5** was tested for its suitability to form homopolymers. It was subjected to a Yamamoto reaction employing nickel(0) and 2,2'-bipyridine (Figure 2a), which resulted in the poly(BODIPY) **P1** in 95% yield. In the next step, dye monomer **5** was utilized for the preparation of alternating copolymers. For that purpose, **5** was copolymerized with 1,4-diethynylbenzene (**6**) in the presence of copper iodide and (PPh₃)₂Pd(II)Cl₂, i.e., Hagihara–Sonogashira reaction conditions (Figure 2b). The high-molecular-weight material **P2** was obtained in 80% yield. In a second copolymerization, **5** was reacted with benzene-1,4-diboronic acid (**7**) as comonomer and (PPh₃)₄-Pd(0) as the catalyst (Figure 2c). This Suzuki polycondensation resulted in the poly(BODIPY) **P3**, obtained in 23% yield.

The results of homo- and copolymerizations are summarized in Table 1. TGA revealed that all three polymers, **P1**,

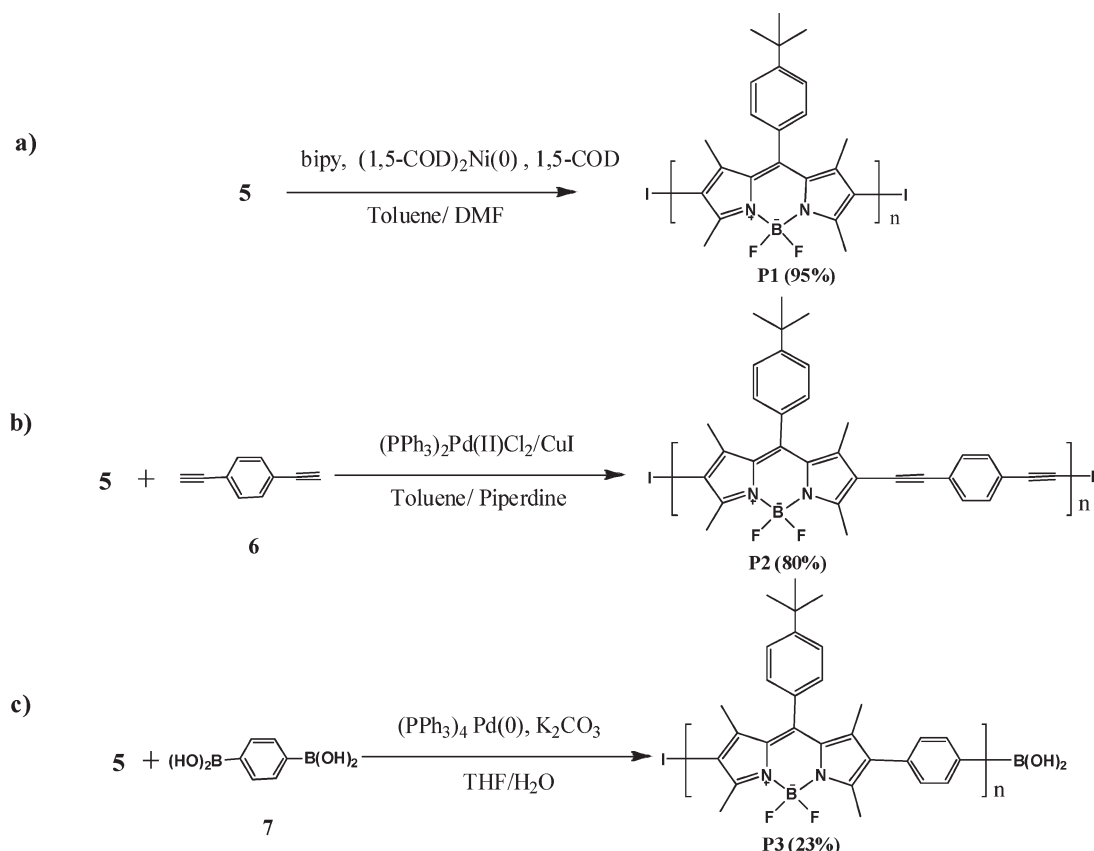


Figure 2. Synthetic route to the poly(BODIPY)s.

P2, and **P3**, exhibit a high thermal stability. No decompositions for **P1**, **P2**, and **P3** were detected up to 345, 360, and 320 °C, respectively. The conjugated polymers poly(BODIPY) **P1** and **P2** were well soluble in organic solvents such as chloroform and THF. However, **P3** was only partially soluble in these solvents. This might be due to aggregation of the polymeric units that exhibit extended π -systems. Larger or additional bulky alkyl groups at the benzene ring within **5** or within monomer **7** might be necessary to increase the solubility of polymers of type **P3**. Another indication of the efficient π - π -stacking of **P3** is revealed by the GPC results. The molecular weight of **P3** is lower than for **P1** and **P2**. Moreover, the homopolymerization of **5** yielded polymeric materials with significantly higher molecular weight than the copolymerizations. This can be explained by the fact that both the Hagihara–Sonogashira as well as the Suzuki polycondensation are experimentally more demanding than the Yamamoto method. In the former reactions, the 1:1 molar equivalence of the complementary reactive functionalities must be adhered to precisely, while in the latter the monomer has intrinsic stoichiometric balance, which is crucial for high molar mass polymer synthesis according to Carother's equation.^{33,34} This holds especially true for small entries as employed herein. Another point that must be explicitly addressed here is that the calculated molecular weights based on polystyrene (PS) standards in Table 1 do not represent the real molecular weights of **P1**, **P2**, and **P3**, as the rigid backbone of these polymers induces different elution behavior than that of conformationally flexible PS. The polydispersities D of homo- and copolymers are narrow for typical polycondensation reactions. D ranges from 3.02 to 3.48 for **P3** and **P1**, respectively. Finally, the NMR data for **P1**, **P2**, and **P3** are consistent with the proposed polymer structures.

Table 1. Molecular Weight, Polydispersity, and Thermogravimetric Analysis Data for the Polymers **P1** to **P3**

polymer	M_n^a (g/mol)	M_w^a (g/mol)	D^a	TGA ^b (°C)
P1	22 300	77 600	3.48	345
P2	9 700	30 600	3.15	360
P3	6 400	19 300	3.02	320

^a Molar mass (M_n , M_w) and polydispersity (D) were determined by GPC in THF against polystyrene standards with UV detection set at absorption maxima. ^b TGA data show the temperature for onset of the primary mass loss.

Table 2. Optical Properties of the BODIPY Monomers **4** and **5** as well as the Polymers **P1** to **P3**

compound	absorption λ_{\max} (nm)	ϵ (M ⁻¹ cm ⁻¹)	emission λ_{\max} (nm)	ϕ_f^a
4	500	47 000	513	0.71
5	530	45 400	544	0.02
P1	503	475 000	510	0.57
P2	325	107 500	385	0.03
P3	535	20 000	575	0.24

^a The fluorescence quantum efficiency was measured against the standard Rhodamine B.¹⁹

Optical Properties. The photophysical properties of the BODIPY polymers and of their low-molecular-weight precursors are summarized in Table 2. The non-halogenated dye **4** showed a high absorption coefficient (ϵ) of 47 000 M⁻¹ cm⁻¹ and a quantum efficiency of fluorescence (ϕ_f) of 0.71 in ethanol. ϵ of the BODIPY monomer **5** was, at 45 400 M⁻¹ cm⁻¹, similar to that of **4**. However, a much lower quantum efficiency of fluorescence was detected for **5** (ϕ_f = 0.02), suggesting that the intersystem crossing efficiency from the lowest singlet excited state to the triplet state was enhanced by the internal heavy-atom effect.^{35,36} The iodination of

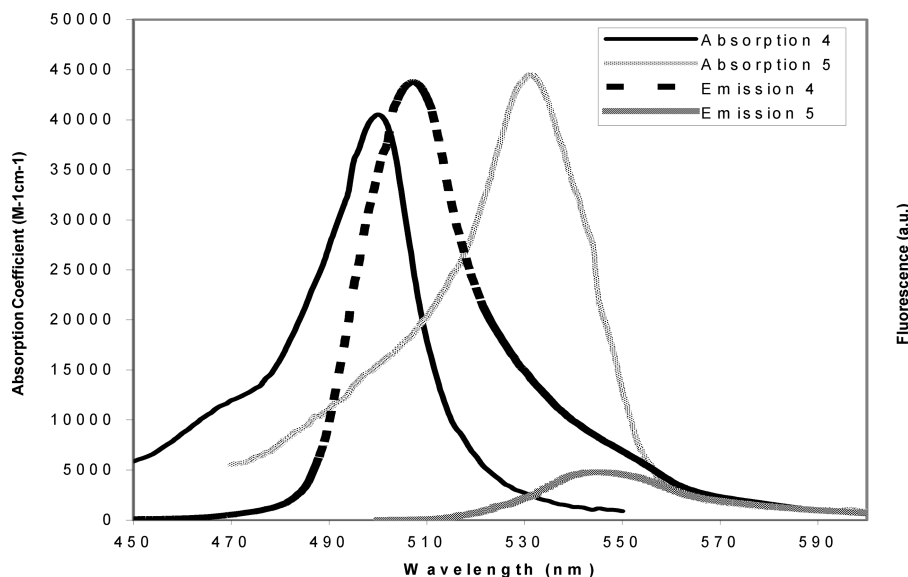


Figure 3. Absorption and emission spectra of compounds **4** and **5**.

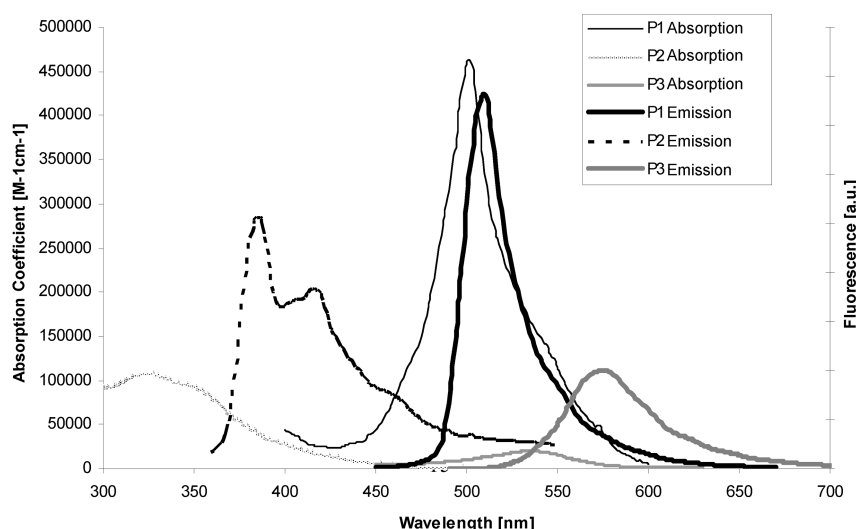


Figure 4. Absorption and emission spectra of **P1**, **P2**, and **P3**.

BODIPY dye **4** also influenced the absorption and emission behavior. The non-halogenated compound **4** exhibits absorption and emission maxima at 500 and 513 nm, respectively (Figure 3). For monomer **5** the respective maxima were shifted to the red by 30 nm (absorption $\lambda_{\text{max}} = 530$ nm, fluorescence $\lambda_{\text{max}} = 544$ nm) (Figure 3).

Looking at the polymers, **P1** exhibited an absorption maximum at 503 nm and a narrow emission spectrum with a maximum at 510 nm when excited at 502 nm (Figure 4). Since the absorption and emission behavior were very similar to that of BODIPY dye **4**, it was assumed that there is little electronic interaction between the chromophoric units along the polymer chain. That could be explained by a perpendicular arrangement of the BODIPY dyes within the backbone induced by the methyl groups in the 1-, 3-, 5-, and 7-positions of the boron-*s*-indacene scaffold. **P2**, wherein the BODIPY dye is connected by diethynylbenzene units, showed an absorption maximum at 325 nm (Figure 4). The emission band exhibited a maximum at 385 nm followed by two vibronic side bands at 415 and 462 nm. Interestingly, **P3**, which was composed of alternating BODIPY and benzene units, showed broad absorption and emission bands with

maxima at 535 and 575 nm, respectively (Figure 4). The broad signals could again be explained by aggregation of polymer chains even in dilute solutions. More important is that by choosing two different comonomers the absorption and emission properties can be significantly manipulated with respect to the homopolymer **P1**, achieving a hypsochromic and bathochromic shift, respectively. Further investigations of the emissive properties of the poly(BODIPY) polymers revealed that the homopolymer **P1** exhibited a higher fluorescence quantum yield (57%) than the copolymers **P2** (3%) and **P3** (24%) (Table 2).

To elucidate the emissive properties of the poly(BODIPY)s further, single-molecule spectroscopy studies were undertaken.

Single-Molecule Spectroscopy. For polymer **P1** we found that excitation at longer wavelengths, i.e., at 532 nm, resulted in a red-shifted maximum of the fluorescence to about 570 nm (data not shown), indicative of spectral heterogeneity of the polymer. To identify the spectral distribution of the conjugated poly(BODIPY) chromophores, the polymer **P1** was diluted in toluene and transferred to a 10 μm thin sealed microscopic chamber. Confocal single-molecule detection of

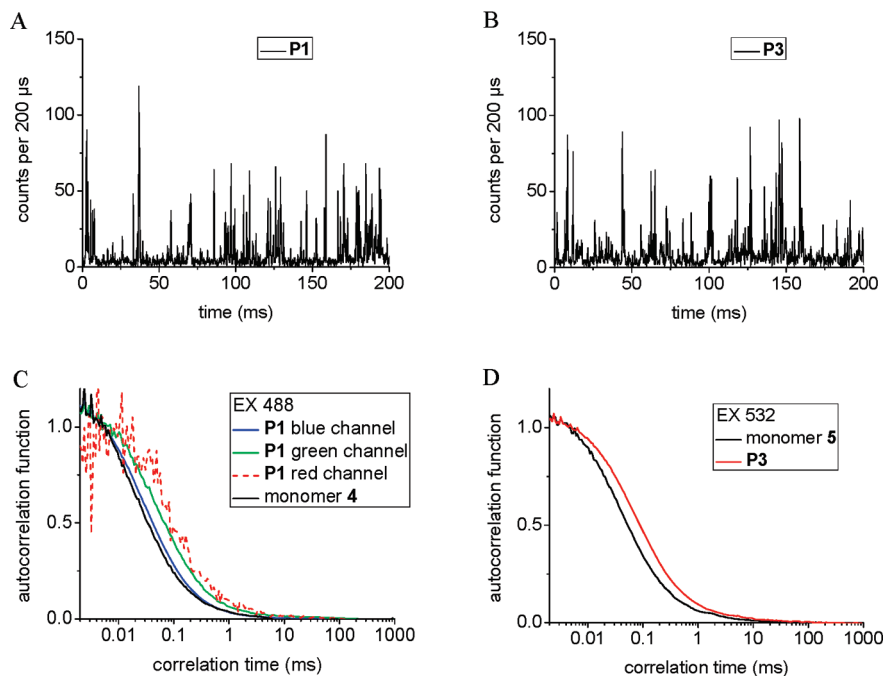


Figure 5. Fluorescence time trajectories and autocorrelation functions (FCS) of freely diffusing single **P1** and **P3** molecules. (A) **P1** in toluene (excitation at 532 nm with 150 μ W, fluorescence detection at 545–625 nm). (B) **P3** in toluene (excitation at 532 nm with 150 μ W, fluorescence detection at 545–625 nm). Photon binning interval is 200 μ s. (C) Spectrally resolved FCS of **P1** with excitation at 488 nm and simultaneous fluorescence detection at $I_{\text{blue}} = 530\text{--}568$ nm (blue curve), $I_{\text{green}} = 575\text{--}625$ nm (green curve), and $I_{\text{red}} > 630$ nm (red curve). (D) FCS of **P3** (excitation at 532 nm, fluorescence detection at 545–625 nm).

freely diffusing **P1** was achieved by laser excitation at 488 or 532 nm. Bursts of photons were generated by individual polymers when traversing the detection volume one after another (Figure 5A). To validate the relation between red-shifted fluorescence and increased size of the conjugated chromophore system in **P1**, we measured the diffusion properties of poly(BODIPY) in toluene solution by fluorescence correlation spectroscopy (FCS). The diffusion properties of (bio)polymers depend on size,²⁵ shape,³⁷ conformation,³⁸ and association with other molecules.³⁹ Here, fluorescence photons were recorded in up to three spectral ranges simultaneously. Exciting the monomer **4** at 488 nm resulted in diffusion times of about 24 ± 6 μ s (mean \pm standard deviation σ) for the spectral range $I_{\text{blue}} = 530\text{--}568$ nm and 30 ± 4 μ s for $I_{\text{green}} = 575\text{--}625$ nm. The mean diffusion times of **P1** increased from 32 ± 5 μ s (I_{blue}) to 50 ± 7 μ s (I_{green}) up to 62 ± 6 μ s ($I_{\text{red}} > 630$ nm) as shown in Figure 5C.

The longer diffusion times of **P1** apparently corresponded to a red-shifted absorbance and a corresponding red-shifted emission. From the relative increase in the diffusion times of **P1**, the apparent mean molecular size of the polymer was estimated using the Stokes–Einstein equation assuming spherical shape. The diffusion times of most red-shifted fluorescent **P1** molecules were increased by a factor of up to 3.7 relative to the diffusion times of blue-shifted monomer **4**. This corresponded to an increase in molecular weight by roughly a factor of 50, i.e., 50 repeating monomer units, which is in reasonable agreement with the GPC data (Table 1).

FCS analysis also provided the mean brightness per molecule as the ratio of the mean fluorescence intensity (in a spectral range) to the mean number of fluorescent molecules in the confocal volume. After excitation at 488 nm with 150 μ W, the mean brightness of a single **P1** in the blue-shifted fluorescence range I_{blue} was 54 ± 5 kHz (mean \pm standard deviation σ), i.e., about 20% higher than for monomer **4** with 43 ± 3 kHz. However, in the green spectral range, I_{green} , fluorescence of polymer **P1** (14 ± 2 kHz) was 47% brighter

than monomer **4** (9 ± 2 kHz). This effect was more pronounced after excitation at 532 nm, which resulted in photon count rates of 195 ± 15 kHz (mean \pm standard deviation σ) for **P1**. Moreover, in the spectral range $I_{\text{green}} = 545\text{--}625$ nm, the brightness of **P1** in toluene was 6.4 times higher than that of Rhodamine 6G (36 ± 3 kHz) in water with a fluorescence quantum yield of 0.95. This indicates that several independent fluorescent chromophoric systems coexist within a single **P1** polymer chain.

When multiple chromophores are contained within a single polymer, internal fluorescence resonance energy transfer (FRET) between the blue- and red-shifted chromophoric systems can occur. FRET is generally associated with a shortening of the fluorescence lifetime, specifically of the blue-shifted chromophores acting as FRET donors. To evaluate internal FRET, we assigned individual **P1** molecules to two subclasses by their respective spectral ratio R . Using pulsed excitation at 488 nm and fluorescence detection in the range $I_{\text{blue}} = 530\text{--}568$ nm and $I_{\text{green}} = 575\text{--}625$ nm, molecules with $R < 0.4$ showed fluorescence lifetimes of 3.2 ns in the I_{blue} range and 2.6 ns in the I_{green} range. The fluorescence lifetimes of monomer **4** were 3.0 ns for both spectral ranges. For **P1** molecules with $R > 0.4$, shortened fluorescence lifetimes suggestive of FRET were found, 2.9 ns in the I_{blue} range and 2.5 ns in the I_{green} range. However, these fluorescence lifetime differences were nonetheless small compared to photonic wires with strong FRET.^{40,41}

The diffusion and brightness properties of polymer **P3** and monomeric compound **4** were similarly measured in toluene solution. Using 532 nm excitation and fluorescence detection in two spectral ranges, we found an increase in diffusion time from 42 ± 4 μ s for monomer **4** to 74 ± 5 μ s for **P3**, i.e., by a factor 1.8 (Figure 5D). Accordingly, the mean molecular size for the polymer **P3** was estimated to contain 6 monomeric units, lower than expected from the GPC data. The mean brightness of a single **P3** molecule, 147 ± 15 kHz, was slightly lower than that of **P1**. Thus, fluorescence was 2 times

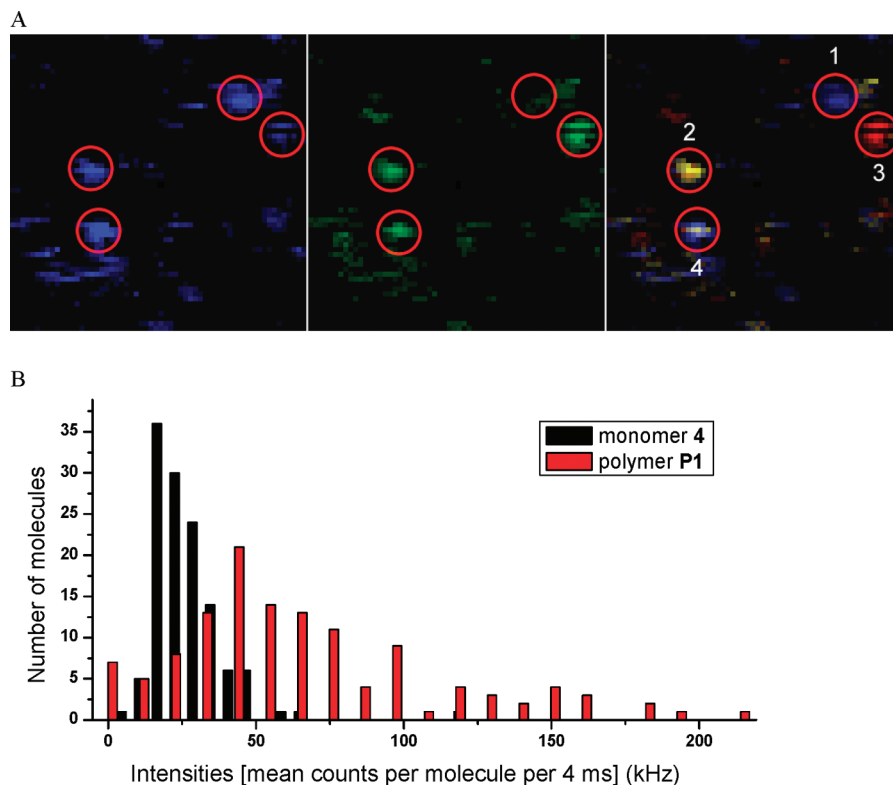


Figure 6. (A) Spectrally resolved confocal images of single polymer **P1** molecules spin-coated on glass (excitation at 488 nm with 10 μ W). Fluorescence is recorded in the blue spectral channel, $I_{\text{blue}} = 530\text{--}568$ nm (left image), and simultaneously in the green channel, $I_{\text{green}} = 575\text{--}625$ nm (middle). The calculated false-color image (right) of polymer **P1** is color-coded by the spectral ratio $R = I_{\text{green}} / (I_{\text{blue}} + I_{\text{green}})$, with bluish pixels corresponding to R around 0.25, yellow pixels with ratio 0.45, and red pixels with ratio 0.63. Images consist of 30×30 pixels with 67 nm pixel size. The four selected **P1** molecules are discussed in the text. (B) Mean fluorescence intensities per single monomer **4** and **P1** molecule, respectively.

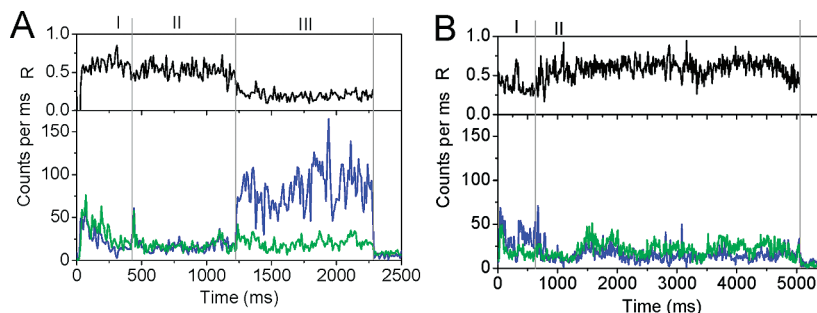


Figure 7. Spectral fluctuations in single **P1** molecules spin-coated onto a glass surface (excitation at 488 nm with 10 μ W). (A) Molecule 1 jumps from red-shifted fluorescence in state I to intermediate state II and to a blue-shifted state III before photobleaching. (B) Molecule 2 jumps from blue-shifted fluorescence (state I) at the beginning to red-shifted but also fluctuates within state 2 before photobleaching.

brighter than Rhodamine 6G, again indicating the presence of more than a single chromophoric system in the polymer chain of **P3**.

To identify the dynamics of the spectral distribution of the conjugated poly(BODIPY) chromophores, single molecules of **P1** spin-coated on glass were imaged by confocal microscopy (Figure 6). Simultaneous detection of the fluorescence intensities in three spectral ranges ($I_{\text{blue}} = 530\text{--}568$ nm, $I_{\text{green}} = 575\text{--}625$ nm, $I_{\text{red}} > 630$ nm) showed different contributions in these spectral ranges for individual polymers. After calculating the red shift of each fluorescence spectrum by the spectral ratio $R = I_{\text{green}} / (I_{\text{blue}} + I_{\text{green}})$ the false-colored single **P1** molecules appeared as round spots consisting of several pixels. Bluish spots correspond to **P1** with a fluorescence maximum between 500 and 550 nm (see molecule 1). Yellowish spots indicate a fluorescence maximum around 570 nm (molecule 2), and red spots relate to a

maximum $\lambda_{\text{EM}} > 590$ nm (molecule 3) in the color coding in Figure 6A.

Compared to single monomer **4** on glass surface, a significantly larger fraction of polymer **P1** molecules exhibited a red-shifted fluorescence spectrum. In addition, the distribution maximum of the mean fluorescence intensities of individual **P1** molecules was shifted to a higher brightness (Figure 6B). Some **P1** molecules emitted up to 10 times more photons than the average single monomer **4** when excited with the same laser power at 488 nm. The photophysical stability of individual **P1** was high; most of the molecules did not bleach within 5 s. However, the fluorescence spectra of some polymers (see molecule 4 in Figure 6A) changed during the confocal sample scanning.

The temporal behavior of the fluctuating red-shifted fluorescence of single **P1** was monitored in spectrally resolved time trajectories. Only a small number of **P1**

molecules showed spectral jumps of the spectra as shown in Figure 7. The stepwise shift of the fluorescence spectrum of **P1** molecule 1 toward a more bluish fluorescence occurred after 600 ms before it photobleached at 2.2 s. **P1** molecule 2 showed a bluish fluorescence and jumped after 500 ms to a yellowish fluorescence, which slightly fluctuated during the remaining seconds before photobleaching.

Conclusion

We have introduced a new class of polymeric dyes based on the BODIPY chromophore. The introduction of two iodine functionalities into the 4-bora-3a,4a-diaza-s-indacene scaffold resulted in a dye monomer that could be efficiently homo- and copolymerized via transition-metal-catalyzed reactions to form high-molecular-weight materials. The nickel-mediated Yamamoto reaction resulted in poly(BODIPY) homopolymers with a high degree of polymerization, while somewhat lower molecular weights of copolymers were obtained via the palladium-catalyzed Suzuki and Hagihara–Sonogashira cross-coupling reactions. The photophysical properties of the polymeric dyes were investigated extensively in bulk and on the single molecule level. The absorption and emission wavelengths of the BODIPY homopolymer **P1** were very similar to that of the monomeric dye. In contrast, efficient color-tuning was achieved by copolymerization. When conjugated comonomers were introduced to form alternating BODIPY copolymers **P2** and **P3**, the absorption and emission wavelengths could be significantly shifted to the blue and to the red, respectively. The homopolymer **P1** showed a high fluorescence quantum yield of 57%, which is remarkable in the context of polymeric dyes emitting at that wavelength.

Single-molecule spectroscopy in solution confirmed the very high brightness of individual **P1** and **P3** polymers. In particular, following excitation in the long-wavelength region of the absorbance maximum, **P1** fluorescence was several times brighter than a single Rhodamine 6G molecule with a quantum yield near unity. We conclude that within a single poly(BODIPY) chain multiple independent chromophoric systems made of multiple conjugated BODIPY dyes can occur. As expected for a polymer with residual flexibility, the number and size of these chromophoric systems fluctuate in time, as shown by spectrally resolved images of individual surface-bound **P1**.

The possibility of exciting the chromophoric systems in poly(BODIPY) with a broad range of common laser lines opens the way to a variety of applications. In the future we will direct our efforts to employ the polymeric BODIPY dyes in organic electronic devices and as bright multichromophoric labels for biological applications after rendering them water-soluble.

References and Notes

- Marechal, E. *Prog. Org. Coat.* **1982**, *10*, 251–287.
- Baier, J.; Pösch, P.; Jungmann, G.; Schmidt, H.-W.; Seilmeier, A. J. *Chem. Phys.* **2001**, *114*, 6739–6743.
- Hernando, J.; de Witte, P. A. J.; van Dijk, E. M. H. P.; Korterik, J.; Nolte, R. J. M.; Rowan, A. E.; Garcia-Parajo, M. F.; van Hulst, N. F. *Angew. Chem., Int. Ed.* **2004**, *43*, 4045–4049.
- Becker, S.; Ego, C.; Grimsdale, A. C.; List, E. J. W.; Marsitzky, D.; Pogantsch, A.; Setayesh, S.; Leising, G.; Mullen, K. *Synth. Met.* **2001**, *125*, 73–80.
- Gomez, R.; Veldman, D.; Blanco, R.; Seoane, C.; Segura, J. L.; Janssen, R. A. J. *Macromolecules* **2007**, *40*, 2760–2772.
- Nielsen, C. B.; Veldman, D.; Martin-Rapun, R.; Janssen, R. A. J. *Macromolecules* **2008**, *41*, 1094–1103.
- Ego, C.; Marsitzky, D.; Becker, S.; Zhang, J. Y.; Grimsdale, A. C.; Mullen, K.; MacKenzie, J. D.; Silva, C.; Friend, R. H. *J. Am. Chem. Soc.* **2003**, *125*, 437–443.
- Quante, H.; Schlichting, P.; Rohr, U.; Geerts, Y.; Mullen, K. *Macromol. Chem. Phys.* **1996**, *197*, 4029–4044.
- Former, C.; Becker, S.; Grimsdale, A. C.; Mullen, K. *Macromolecules* **2002**, *35*, 1576–1582.
- Sommer, M.; Lindner, S.; Thelakkat, M. *Adv. Funct. Mater.* **2007**, *17*, 1493–1500.
- Geiger, T.; Benmansour, H.; Fan, B.; Hany, R.; Nuesch, F. *Macromol. Rapid Commun.* **2008**, *29*, 651–658.
- Yamamoto, T.; Kizu, K. *J. Phys. Chem.* **1995**, *99*, 8–10.
- Bartholome, D.; Klemm, E. *Macromolecules* **2006**, *29*, 5646–5651.
- Kawao, M.; Ozawa, H.; Tanaka, H.; Ogawa, T. *Thin Solid Films* **2006**, *499*, 23–28.
- Ulrich, G.; Ziessel, R.; Harriman, A. *Angew. Chem., Int. Ed.* **2008**, *47*, 1184–1201.
- Zhu, M.; Jiang, L.; Yuan, M.; Liu, X.; Ouyang, C.; Zheng, H.; Yin, X.; Zuo, Z.; Liu, H.; Li, Y. *J. Polym. Sci., Part A: Polym. Chem.* **2008**, *46*, 7401.
- Meng, G.; Velayudham, S.; Smith, A.; Luck, R.; Liu, H. *Macromolecules* **2009**, *42*, 1995–2001.
- Treibs, A.; Kreuzer, F. H. *Ann. Chem.* **1968**, *718*, 208–213.
- Haughland, R. P. *Handbook of Fluorescent Probes and Research Products*, 9th ed.; Molecular Probes: Eugene, OR, 2003.
- Hepp, A.; Uirich, G.; Schmechel, R.; von Seggern, H.; Ziessel, R. *Synth. Met.* **2004**, *146*, 11–15.
- Kabac, J.; Jedrzejewska, B.; Orlinski, P.; Paczkowski, J. *Spectrochim. Acta, Part A* **2005**, *62*, 115–125.
- Duser, M. G.; Bi, Y. M.; Zarrabi, N.; Dunn, S. D.; Börsch, M. *J. Biol. Chem.* **2008**, *283*, 33602–33610.
- Heitkamp, T.; Kalinowski, R.; Bottcher, B.; Börsch, M.; Altendorf, K.; Greie, J. C. *Biochemistry* **2008**, *47*, 3564–3575.
- Peneva, K.; Mihov, G.; Herrmann, A.; Zarrabi, N.; Börsch, M.; Duncan, T. M.; Mullen, K. J. *Am. Chem. Soc.* **2008**, *130*, 5398–5399.
- Alemdaroglu, F. E.; Wang, J.; Börsch, M.; Berger, R.; Herrmann, A. *Angew. Chem., Int. Ed.* **2008**, *47*, 974–976.
- Zarrabi, N.; Duser, M. G.; Reuter, R.; Dunn, S. D.; Wrachtrup, J.; Börsch, M. *Proc. SPIE* **2007**, *6771*, 67710F.
- Krebs, F. C.; Nyberg, B. R.; Jørgensen, M. *Chem. Mater.* **2004**, *16*, 1313–1318.
- Nielsen, K. T.; Bechgaard, K.; Krebs, F. C. *Macromolecules* **2005**, *38*, 658–659.
- de Meijere, A.; Diedrich, F. *Metal-Catalyzed Cross-Coupling Reactions*, 2nd ed.; Wiley-VCH: Weinheim, 2004.
- Pei, Q. B.; Yang, Y. *J. Am. Chem. Soc.* **1996**, *118*, 7416–7417.
- Schluter, A.-D.; Wegner, G. *Acta Polym.* **1993**, *44*, 59–69.
- Weder, C.; Wrighton, M. S. *Macromolecules* **1996**, *29*, 5157–5165.
- Cowie, J. M. G. *Polymers: Chemistry and Physics of Modern Materials*; International Textbook: Aylesbury, England, 1973.
- Schluter, A. D. *J. Polym. Sci., Part A* **2001**, *39*, 1533–1556.
- Yogo, T.; Urano, Y.; Ishitsuka, Y.; Maniwa, F.; Nagano, T. *J. Am. Chem. Soc.* **2005**, *127*, 12162–12163.
- Valeur, B. *Molecular Fluorescence: Principles and Applications*; Wiley-VCH: Weinheim, Chichester, 2002.
- Ding, K.; Alemdaroglu, F. E.; Börsch, M.; Berger, R.; Herrmann, A. *Angew. Chem., Int. Ed.* **2007**, *46*, 1172–1175.
- Börsch, M.; Turina, P.; Eggeling, C.; Fries, J. R.; Seidel, C. A. M.; Labahn, A.; Gräber, P. *FEBS Lett.* **1998**, *437*, 251–254.
- Krebstakies, T.; Zimmermann, B.; Graber, P.; Altendorf, K.; Börsch, M.; Greie, J. C. *J. Biol. Chem.* **2005**, *280*, 33338–33345.
- Heilemann, M.; Tinnefeld, P.; Mosteiro, G. S.; Parajo, M. G.; Van Hulst, N. F.; Sauer, M. *J. Am. Chem. Soc.* **2004**, *126*, 6514–6515.
- Heilemann, M.; Kasper, R.; Tinnefeld, P.; Sauer, M. *J. Am. Chem. Soc.* **2006**, *128*, 16864–16875.